

Future perspectives of SAR polarimetry with applications to multi-parameter fully polarimetric pol-sar remote sensing & geophysical stress-change monitoring with implementation to natural disaster assessment and monitoring within the “Pacific Ring of Fire” by implementation of polar & equatorially orbiting satellite sensors

Wolfgang-Martin Boerner¹⁻⁷

In coordination with

Yoshio Yamaguchi², Akinobu Sato², Roichi Sato², Hiroyoshi Yamada²; Alberto Moreira³, Gerhard Krieger³, Andreas Reigber³, Irena Hajsek³, Kostas Papathanassiou³ ; Katsumi Hattori⁴, Josaphat Tetuko Sri Sumantyo⁴, Kun-Shan Chen⁵, Chih-Yuan Chu⁵, Chih-Tien Wang⁵, Jong-Sen Lee⁵ ; Enrico Paringit⁶; Roberto Heru Triharjanto⁷, Mahmud Raimadoya⁷

1 University of Illinois at Chicago, UIC-ECE/CSN, Chicago, IL/USA

2 Niigata University, Electronic Information Engineering, Ikarashi, Niigata, Japan

3 DLR-HR, Oberpfaffenhofen, Bavaria, Germany

4 Chiba University, Earthquake Research Center & CEReS, Chiba, Japan

5 National Central University, NCU-CSR/SR/MRSL, Jhongli, Taoyuan, Taiwan ROC

6 UPD-GE, Diliman, Quezon City, Metro-Manila, Philippines

7 LAPAN, Jakarta; BAC-CEE/RAWG, Jalan Meranti Dramaga Campus, Bogor, Java, Indonesia

WIDEBAND INTERFEROMETRIC SENSING AND IMAGING POLARIMETRY

1

Exploitation of fully polarimetric Satellite POLSAR modes for natural hazard detection and subsequent disaster reduction of SE-Asian/Pacific earthquakes, volcano eruptions and taiphoons – Japan, Taiwan, Philippines and Indonesia

Abstract: The outstanding performance capabilities of the three Satellite POLSAR sensors are well established; and in this exposition the exploitation of the fully polarimetric ALOS-PAL=PPL=SAR mode is demonstrated by implementing the NIIGATA-UNIVERSITY four-scatterer SAR image decomposition with coherency-matrix rotation proving the superior imaging capabilities of the fully polarimetric SAR modes not only for the ALOS-PALSAR L-Band and similarly to the S-Band, C-Band and X-Band. The novel fully polarimetric POL-SAR image processing techniques are then applied to natural hazard detection and subsequent disaster reduction of taiphoons with landslides, volcano eruptions with plume aftereffects & landslides, and of earthquakes with drop-slips experienced within the SE-Asian/Pacific Ring-of-Fire including next to Japan in Taiwan, the Philippines and Indonesia, promoting equatorially orbiting Single and TanDEM L-/S-/X-Band POLSAR sensor deployment.

WIDEBAND INTERFEROMETRIC SENSING AND IMAGING POLARIMETRY

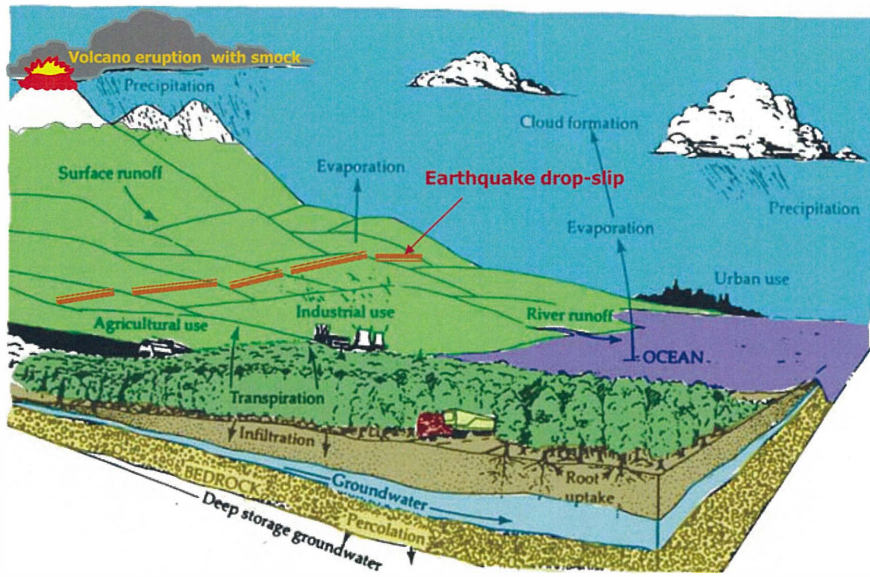
2



Apollo 11: 1969 July 16 - 24

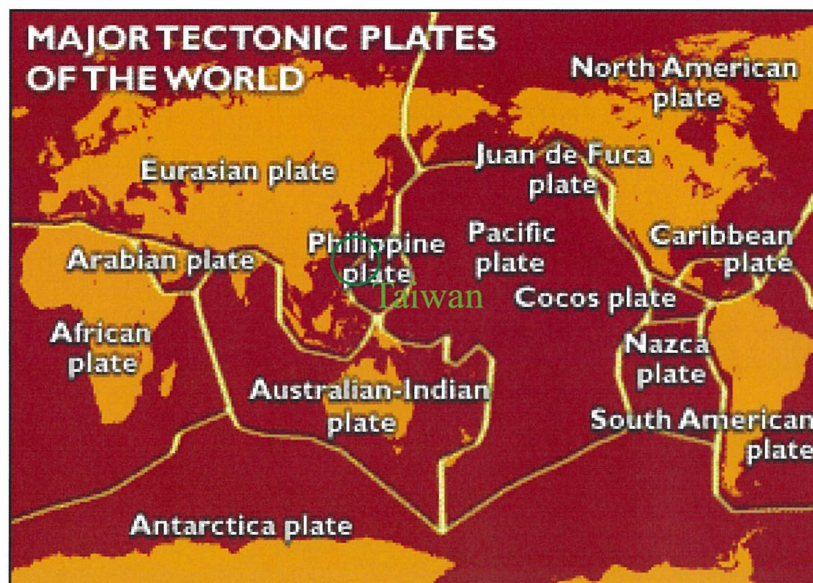


Hydrologic cycle with volcanologic & seismic activity



WIDEBAND INTERFEROMETRIC SENSING AND IMAGING POLARIMETRY

5

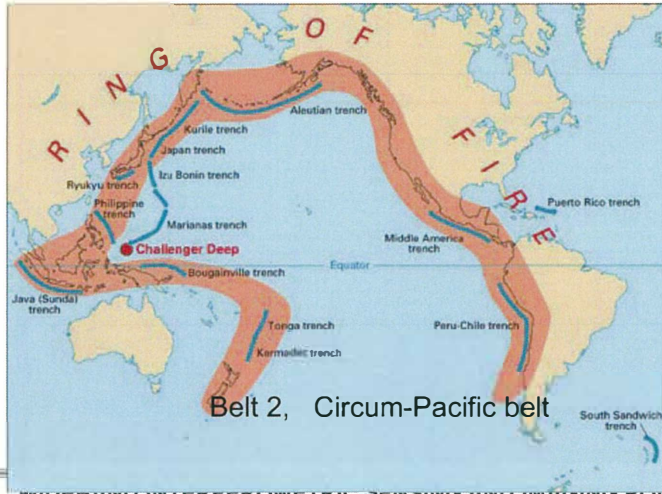


From BBC news site

WIDEBAND INTERFEROMETRIC SENSING AND IMAGING POLARIMETRY

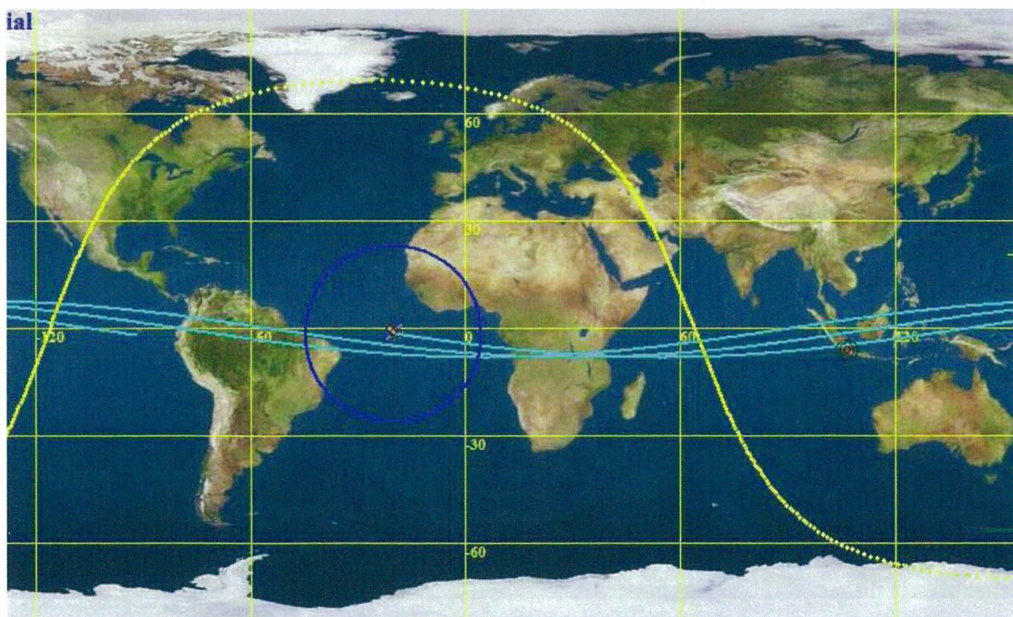
6

The terrestrial tectonology: Alfred Wegener's tectonic plate theory and the two major seismic belts

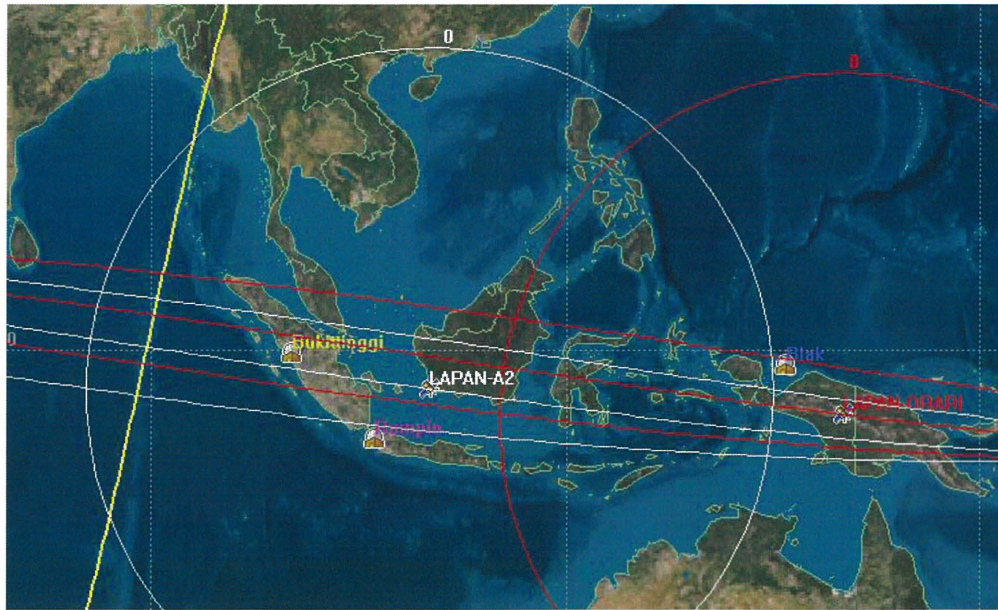


LAPAN-A2 ORBIT PROFILE

(14 pass per 24 hr / orbit time 100 minutes and stay above horizon at about 10 minutes)



TUB-LAPAN-ORARI ORBIT PROFILE
 (14 pass per 24 hr / orbit time 100 minutes and stay above horizon at about 10 minutes)



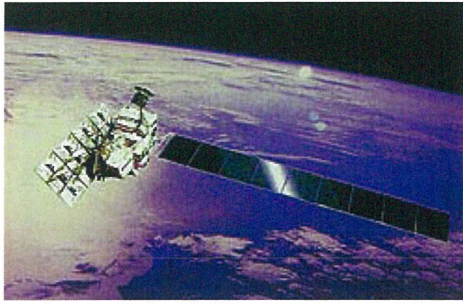
WIDEBAND INTERFEROMETRIC SENSING AND IMAGING POLARIMETRY

Table 1. Comparison of High-Level Parameters

Parameter	PALSAR	RADARSAT-2	TerraSAR-X
Orbit: LEO, circular	Sun-synchronous	Sun-synchronous	Sun-synchronous
Repeat Period (days)	46	24	11
Equatorial Crossing time (hrs)	22:30 (ascending)	18:00 (ascending)	18.00 (ascending)
Inclination (degrees)	98.16	98.6	97.44
Equatorial Altitude (km)	692	798	515
Wavelength (Band)	23 cm (L)	5.6 cm (C)	3 cm (X)
Fully polarimetric mode	Yes	Yes	Yes



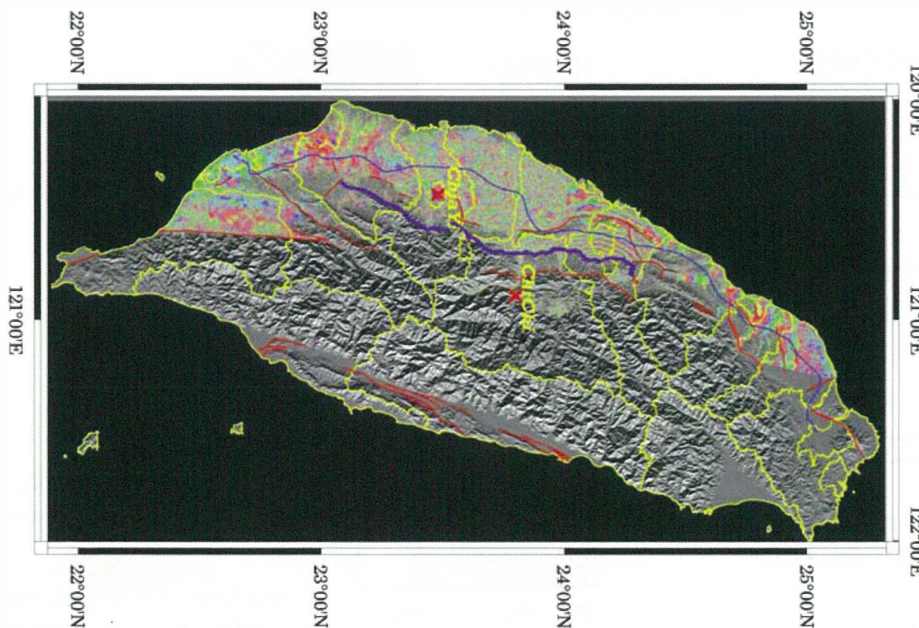
WIDEBAND INTERFEROMETRIC SENSING AND IMAGING POLARIMETRY



ALOS is one of the largest Earth observing satellites ever developed, at 3850 kg. It is in a near-exact 45-day repeat sun-synchronous orbit, 690 km altitude above the equator. The active phased array SAR antenna is obliquely Earth-facing, aligned with the spacecraft velocity vector. The solar array is arranged at right angles to the orbit plane, consistent with the near-mid-day orbit phasing. The X-band down-link must be shared with optical instruments, which constrains SAR operation times.

Table 1. Selected PALSAR Mode Parameters

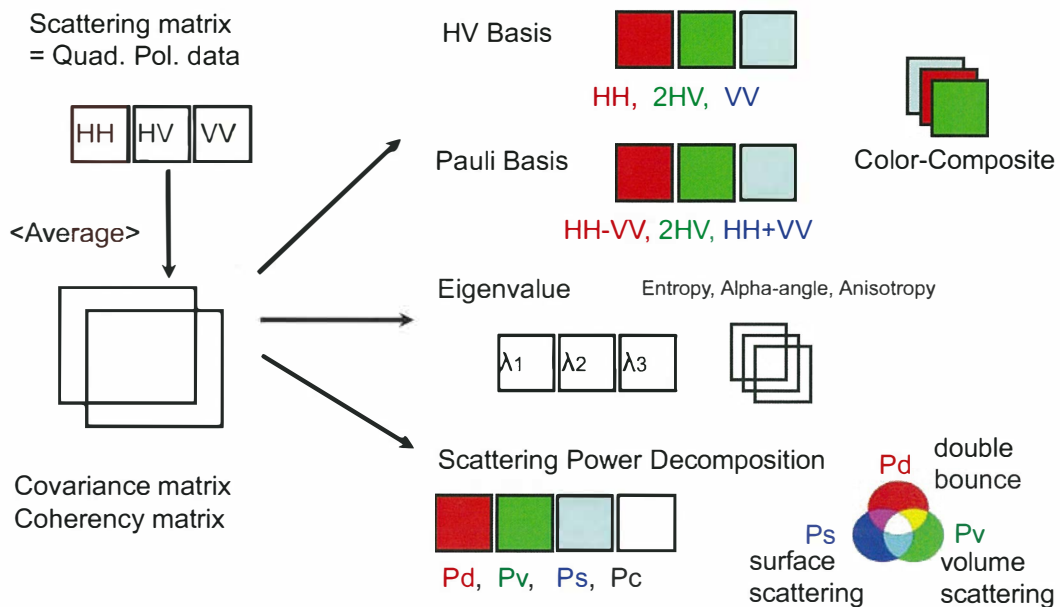
Mode (selected)	Resolution (m)	Swath (km)	Looks	Polarization
Standard, stripmap	20 x 10	70	2	HH or VV
Fine	10	70	1	HH or VV
ScanSAR (5-beam)	~ 100	350	8	HH or VV
Dual polarization	(as above)	(as above)	(as above)	(HH, HV), (VV, VH)
Quad-pol	30 x 10	30	2	Full polarization

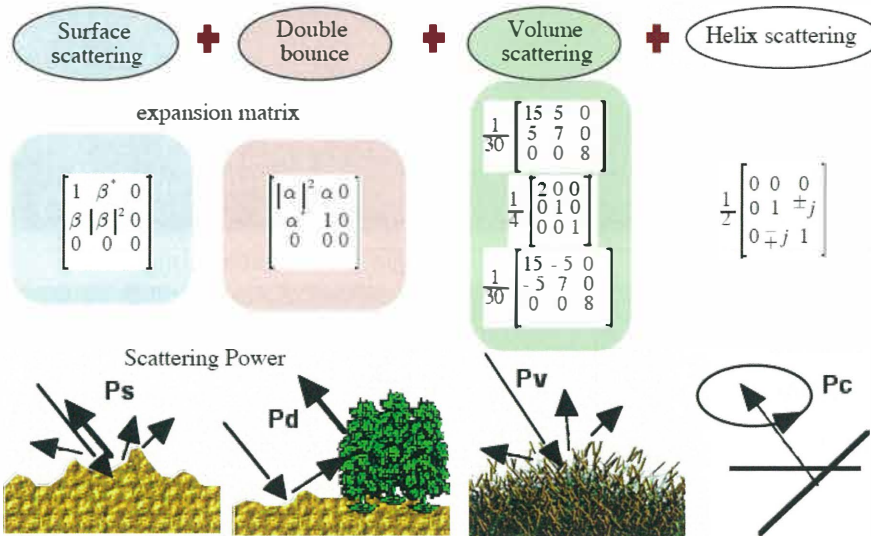




3.4.5.6.7.8
 Polarimetric mode
 Incident angle :23.1°
 Date:2009/05/01
 Path:442
 Frame:430(3),440(4)
 450(5),460(6)
 470(7),480(8)

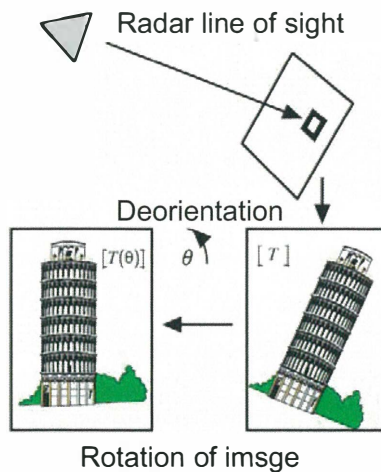
POLSAR image analysis





The four-component decomposition of scattering powers P_s , P_d , P_v , and P_c

4-component scattering power decomposition algorithm using rotated coherency matrix



Taiwan

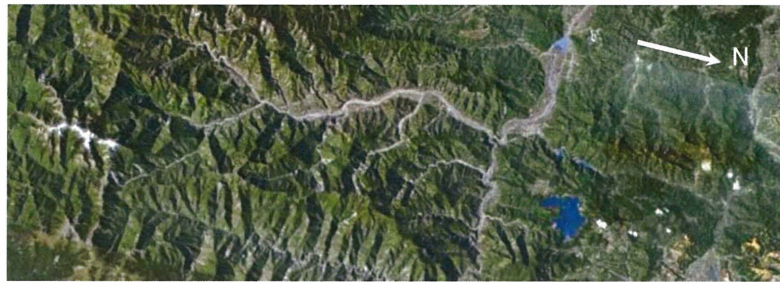
23.703N
120.875E

PASL110090501
14242009070200
02

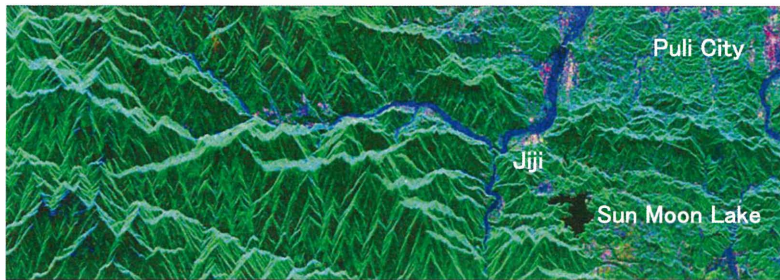


©METI, ERSDAC

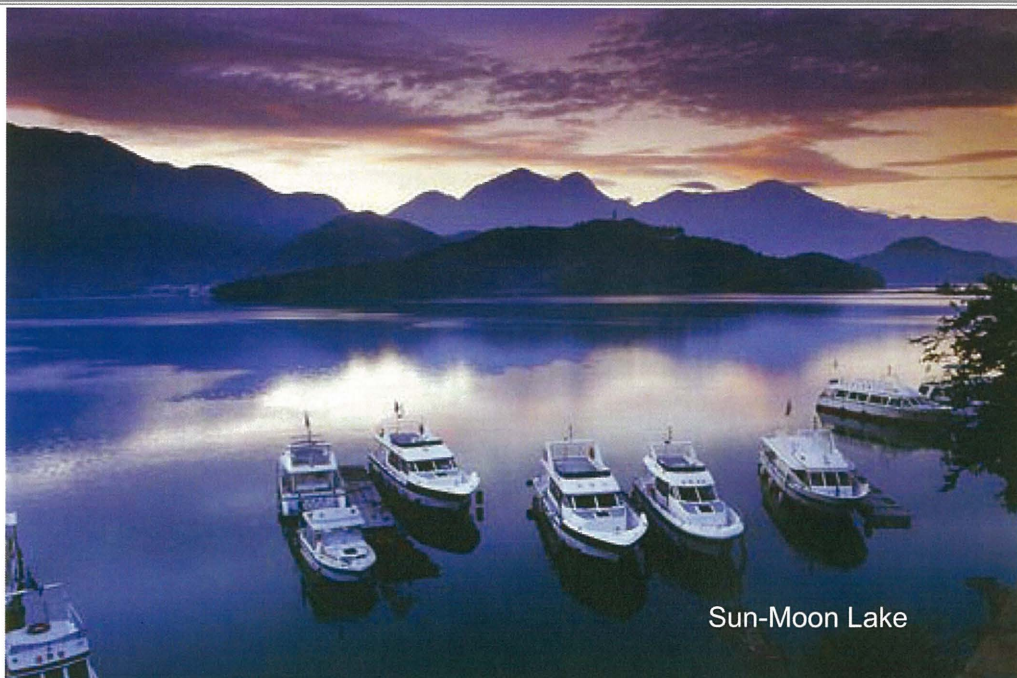
2009/5/1



Google earth optical image

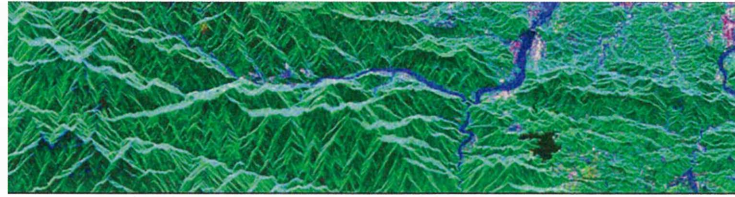


Scattering power decomposition (Pd, Ps, Pv)



Sun-Moon Lake

Scattering power decomposition

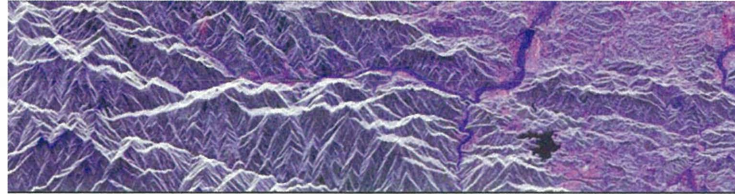


Pd, Pv, Ps

Pauli-basis

Taiwan

23.703N
120.875E



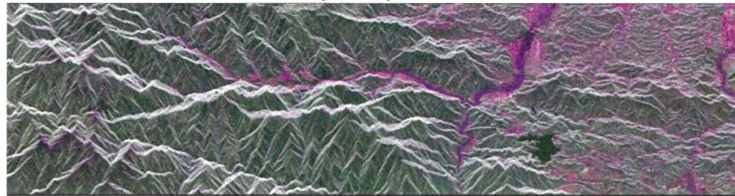
HH-VV, 2HV, HH+VV

HV-basis

2009/5/1

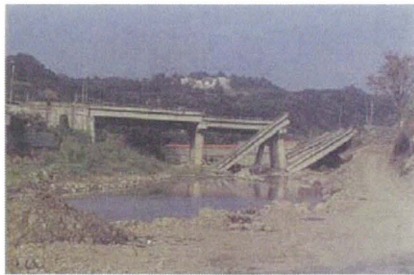
PASL1100905011424200907020002

©METI, ERSDAC



HH, 2HV, VV

The destruction along the Cheleng-Pu fault caused by the Chi-Chi earthquake of 1999 September 21



Scattering power decomposition



T33 Rotation

Pauli-basis

Taiwan

23.703N

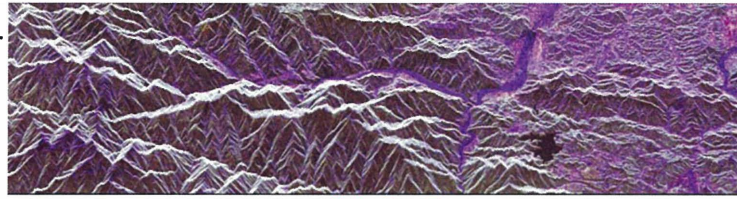
120.875E

HV-basis

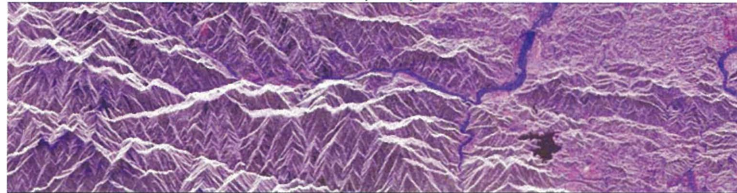
2009/5/1

PASL1100905011424200907020002

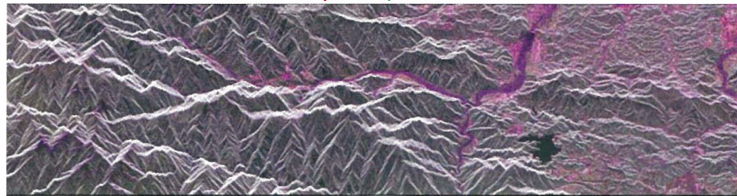
©METI, ERSDAC



Pd, Pv, Ps



HH-VV, 2HV, HH+VV

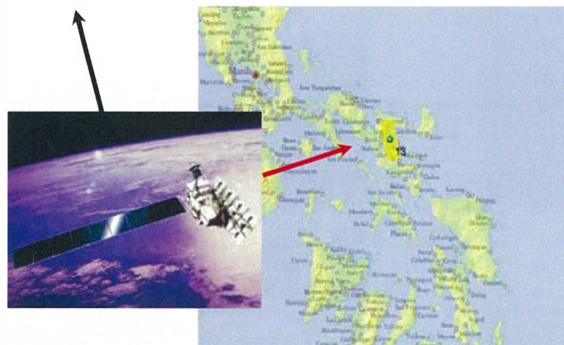


HH, 2HV, VV

ALOS-PALSAR Polarimetric Mode

Philippines

Ascending



13.501N

123.551E

2009/5/30

Data no.
ALPSRP178330
260

© METI, JAXA

Yoshio Yamaguchi





Mt. Mayon – The pearl of the Orient

Philippines

13.498N
123.561E

2010/1/15

Data no.
ALPSRP211880260

©METI, JAXA

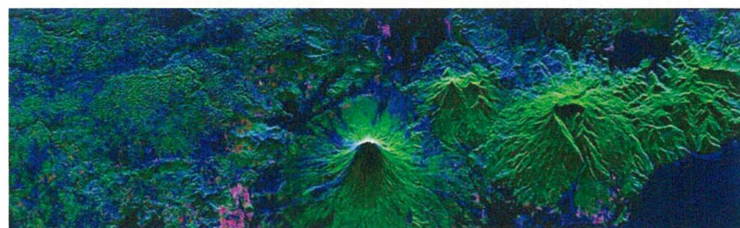
Scattering power
Decomposition



Mt. Mayon

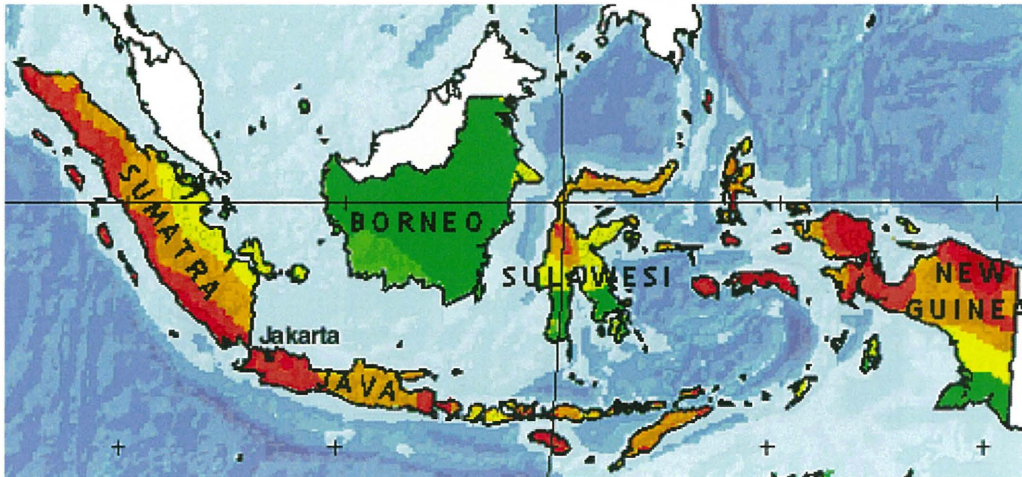


Google Earth optical image



Decomposed image (Ps, Pd, Pv) with rotation 2° window

South-East Asia

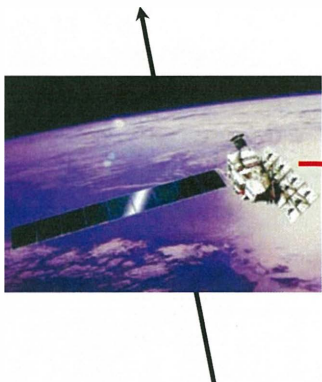


ALOS-PALSAR Polarimetric Mode

Ascending

Indonesia

2007/3/10



Data no.
ALPSRP059887030
ALPSRP059887040

2009/3/15

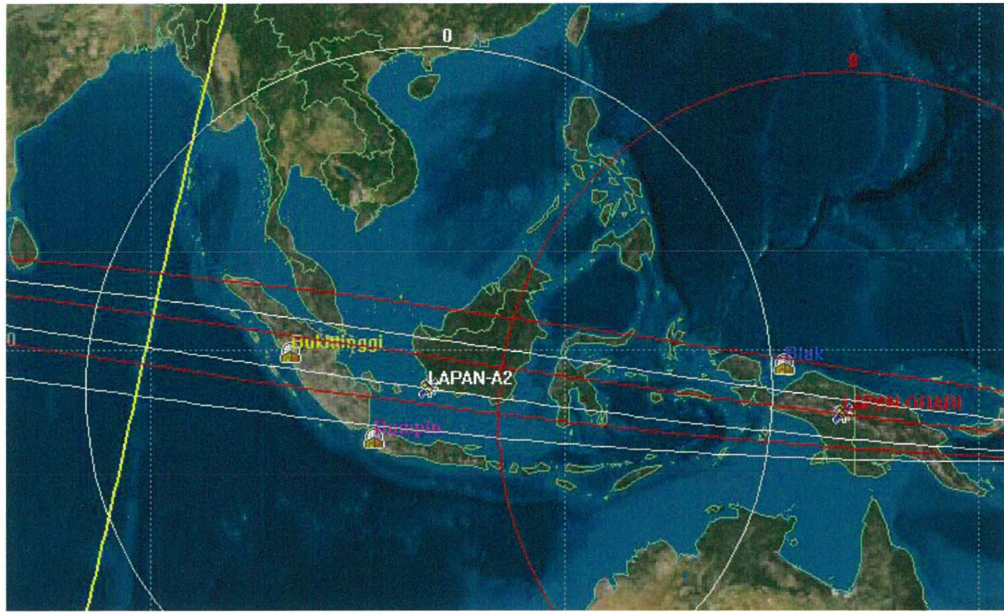
Data no.
ALPSRP167247030
ALPSRP167247040

©JAXA, METI

Yoshio Yamaguchi



TUB-LAPAN-ORARI ORBIT PROFILE
 (14 pass per 24 hr / orbit time 100 minutes and stay above horizon at about 10 minutes)



WIDEBAND INTERFEROMETRIC SENSING AND IMAGING POLARIMETRY

Indonesia

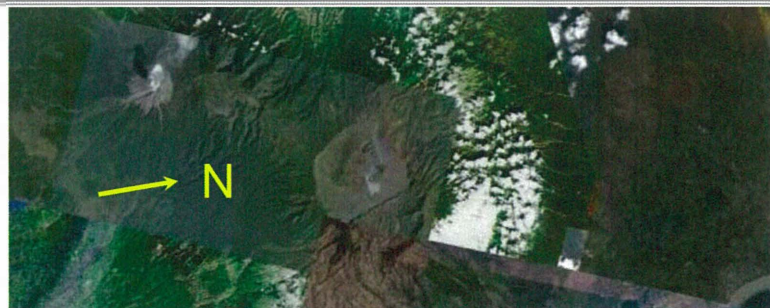
-7.942N
 112.870E

2007/3/10

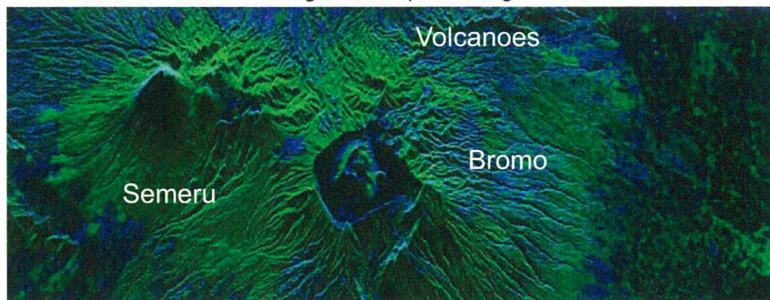
ALPSRP059887030-P1.1_A

©JAXA, METI

Scattering power
 Decomposition



Google earth optical image



Decomposed image (Ps, Pd, Pv)

WIDEBAND INTERFEROMETRIC SENSING AND IMAGING POLARIMETRY



Mount Semeru puffs steam behind a cloud of sulphur gas from Mount Bromo in the Tengger caldera on Java.

Scattering power decomposition



2007/3/10

Pauli-basis

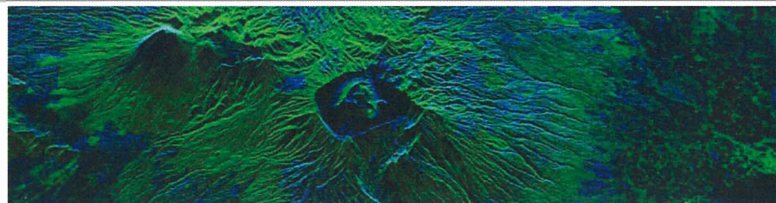
-7.942N

112.870E

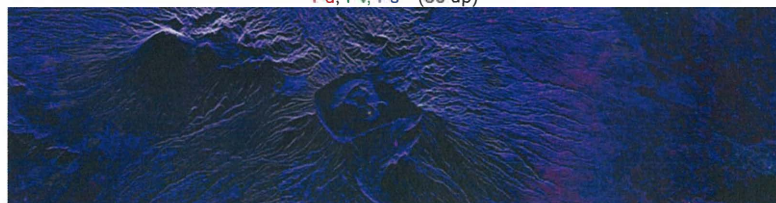
HV-basis
Indonesia

ALPSRP059887030-P1.1__A

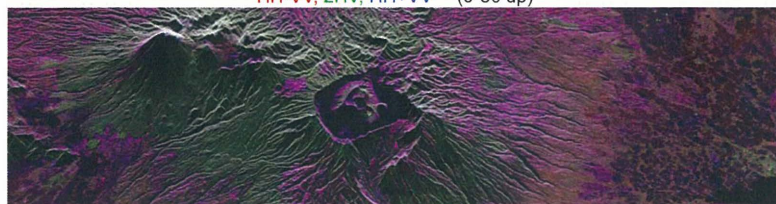
©JAXA, METI



Pd, Pv, Ps (80 up)



HH-VV, 2HV, HH+VV (0-50 up)



HH, 2HV, VV (50 up)

Scattering power decomposition



2007/3/10

T33 Rotation

Pauli-basis

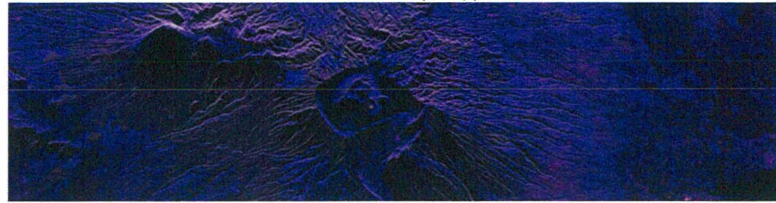
HV-basis

Indonesia
-7.942N
112.870E
ALPSRP059887030-P1.1__A

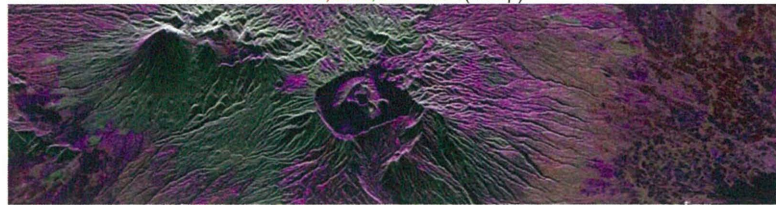
©JAXA, METI



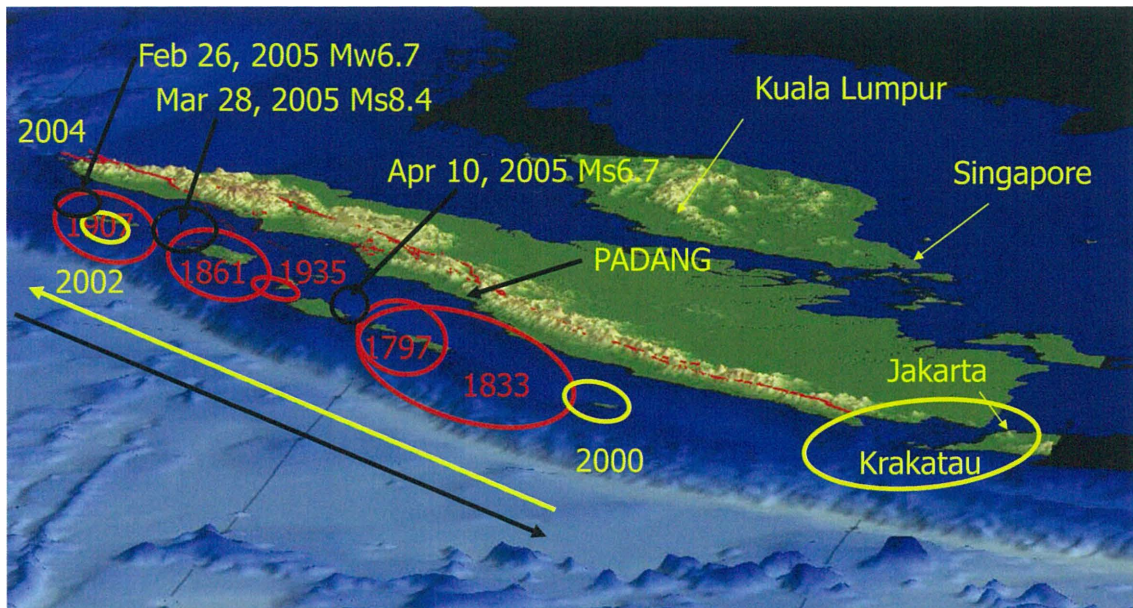
Pd, Pv, Ps (80 up)



HH-VV, 2HV, HH+VV (80 up)



HH, 2HV, VV (50 up)



A flurry of ruptures have occurred since 2000



From Simkin and Fiske, 1983



Krakatau

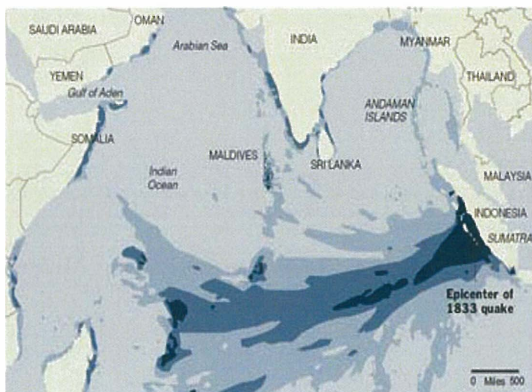


8/26/1883

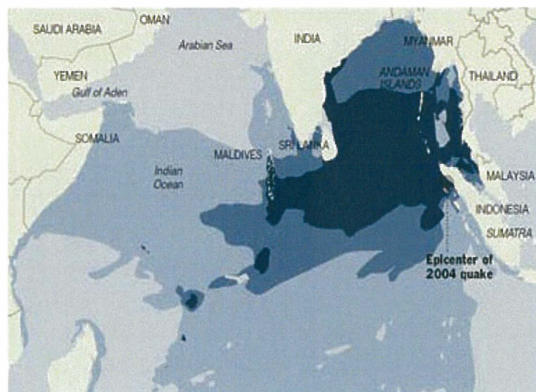


Next major eruption within 20 years

Indian Ocean Tsunamis: 1833 & 2004

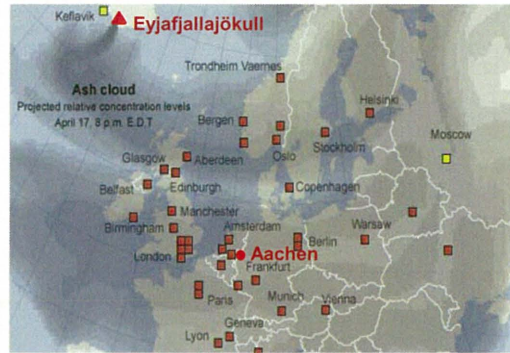
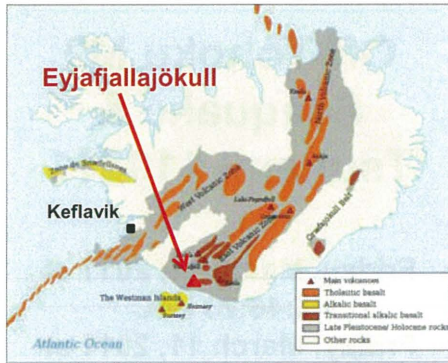


1833 MAXIMUM WAVE HEIGHT OFFSHORE



2004 MAXIMUM WAVE HEIGHT OFFSHORE

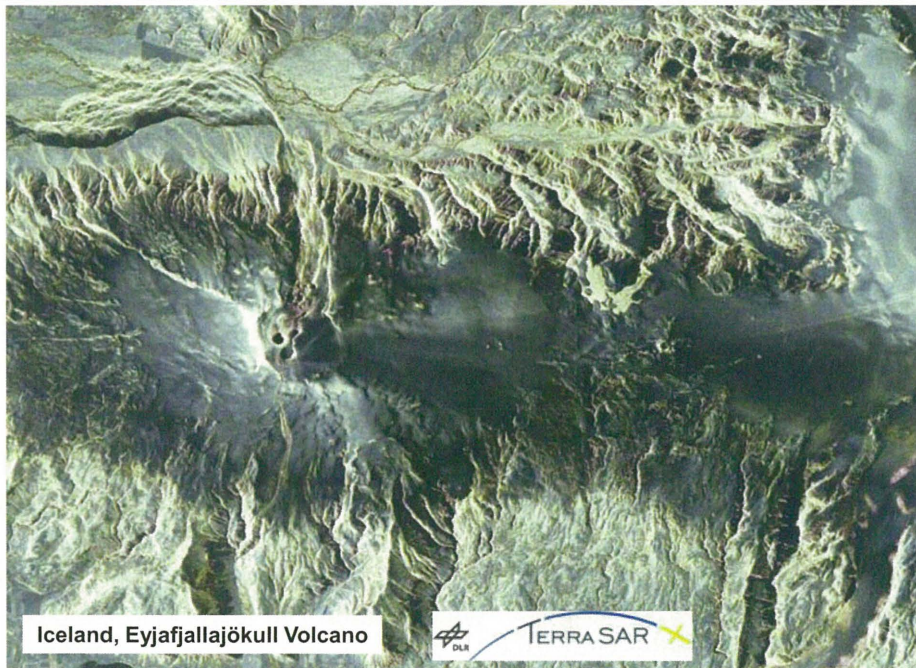
Hannah Fairfield/The New York Times, Science Section, January 4, 2005



Iceland, Eyjafjallajökull Volcano

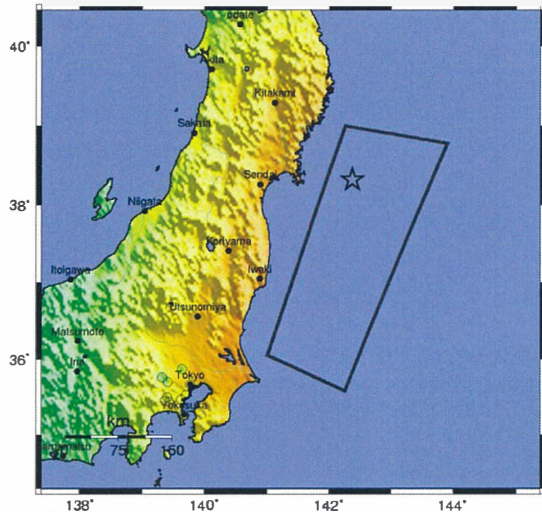


WIDEBAND INTERFEROMETRIC SENSING AND IMAGING POLARIMETRY



WIDEBAND INTERFEROMETRIC SENSING AND IMAGING POLARIMETRY

USGS ShakeMap : NEAR THE EAST COAST OF HONSHU, JAPAN
Fri Mar 11, 2011 05:46:23 GMT M 8.9 N38.32 E142.37 Depth: 24.4km ID c0001 xgp



Map Version 4 Processed Fri Mar 11, 2011 01:23:57 AM MST - NOT REVIEWED BY HUMAN

PERCEIVED SHAKING	Not felt	Weak	Light	Moderate	Strong	Very strong	Severe	Violent	Extreme
POTENTIAL DAMAGE	none	none	none	Very light	Light	Moderate	Moderate-Heavy	Heavy	Very Heavy
PEAK ACC (%g)	< 0.17	.17-1.4	1.4-3.9	3.9-9.2	9.2-18	18-34	34-65	65-124	>124
PEAK VEL. (cms)	<0.1	0.1-1.1	1.1-3.4	3.4-8.1	8.1-16	16-31	31-60	60-116	>116
INSTRUMENTAL INTENSITY	I	II-III	IV	V	VI	VII	VIII	IX	X

Off-Tohoku M9 Seaquake & Tsunami 110311

Friday, March 11, 2011 at
05:46:23 UTC
Friday, March 11, 2011 at
02:46:23 PM at epicenter
Epicenter
38.322°N, 142.369°E

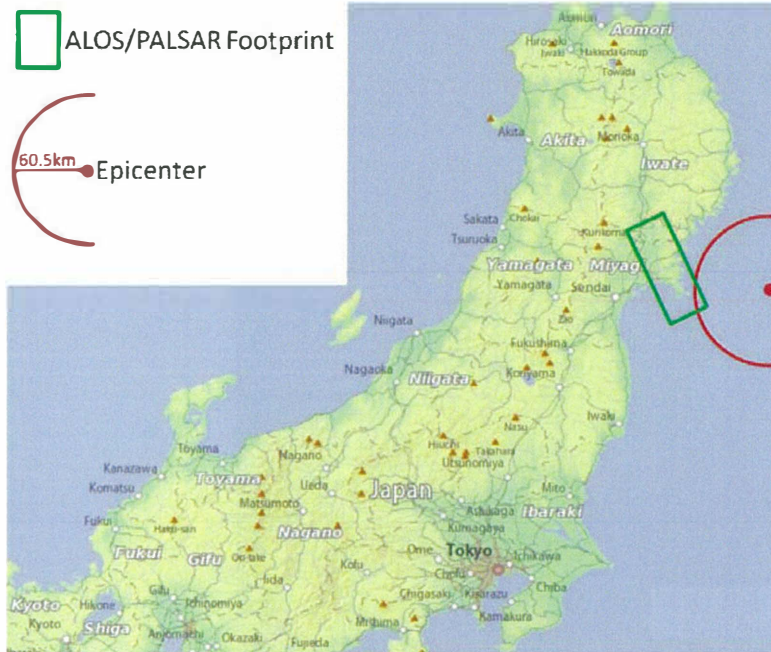


110311-Tsunami OFF-TOHOKU-COASTAL- DISASTER Map-book, 2011 March/April

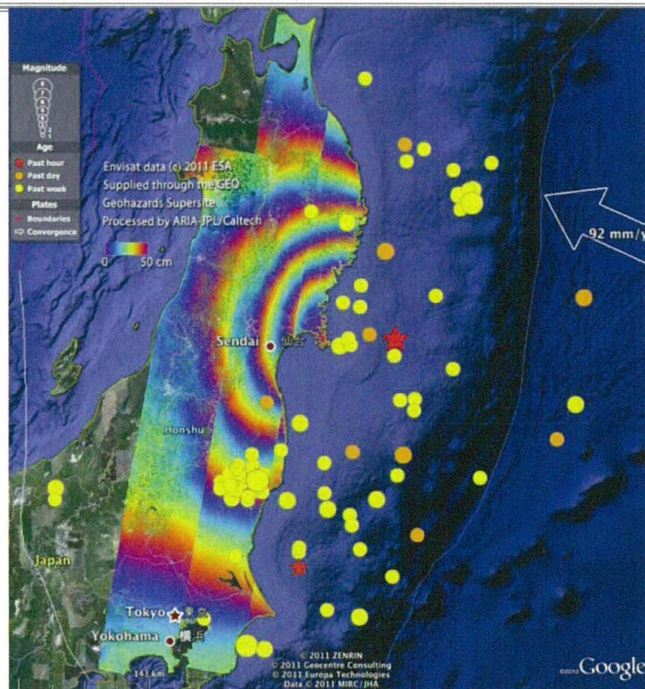
Clearly interpreting the Japanese

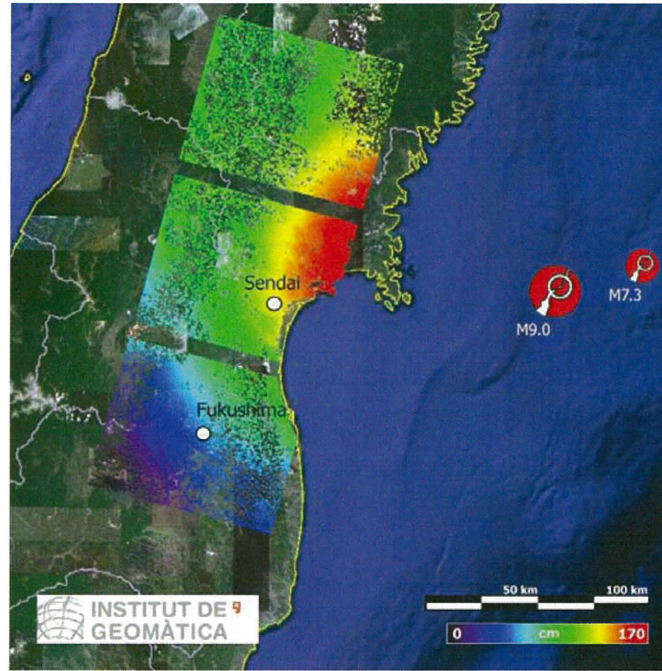
Expression Tsu-nami 津波
= Harbor-wave

Note that every harbor along the affected Eastern Off-Tohoku coastal corridor was severely damaged by the incoming and outgoing tsunami water-walls

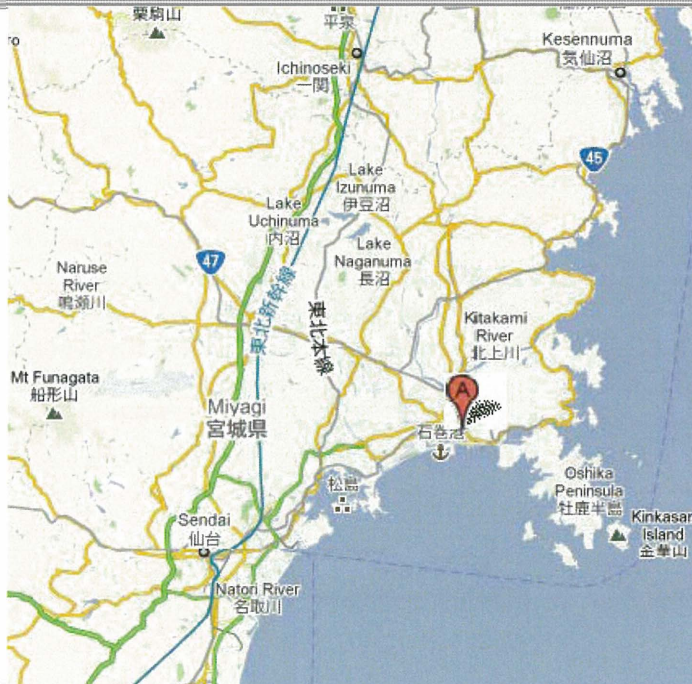


Off-Tohoku 9.0 Earthquake with Super-Tsunami





WIDEBAND INTERFEROMETRIC SENSING AND IMAGING POLARIMETRY



Ishinomaki harbor
38°25'N, 141°18'E

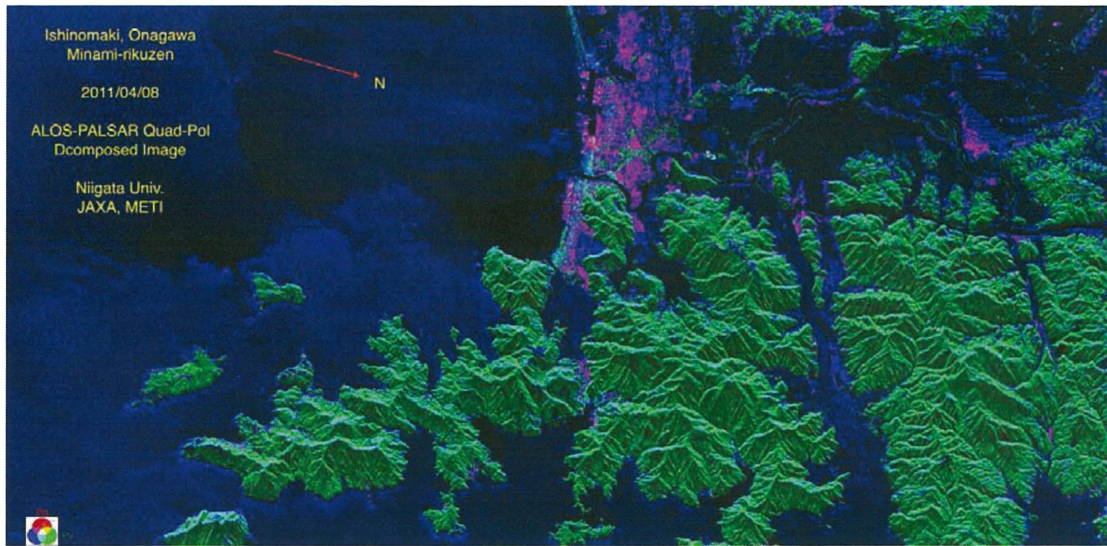
WIDEBAND INTERFEROMETRIC SENSING AND IMAGING POLARIMETRY



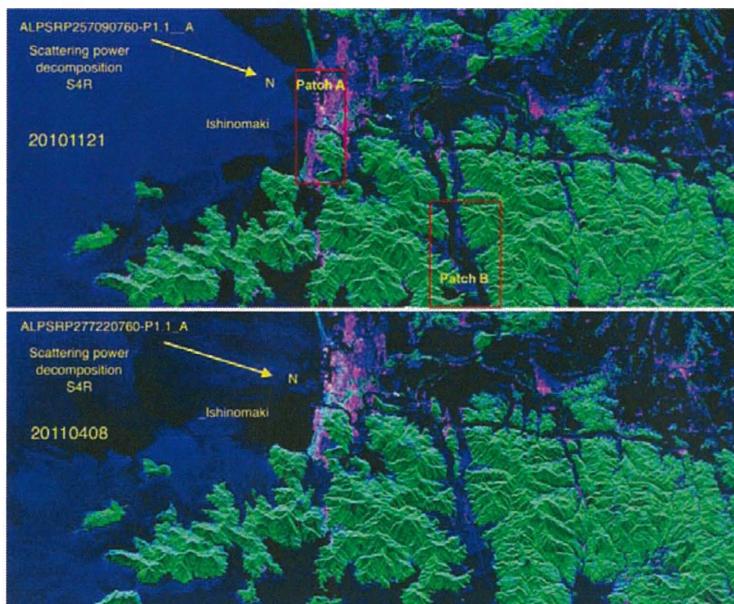
Destruction of City and Harbor of Ishinomaki by 110311 Tsu-nami (Harbor-Wave)



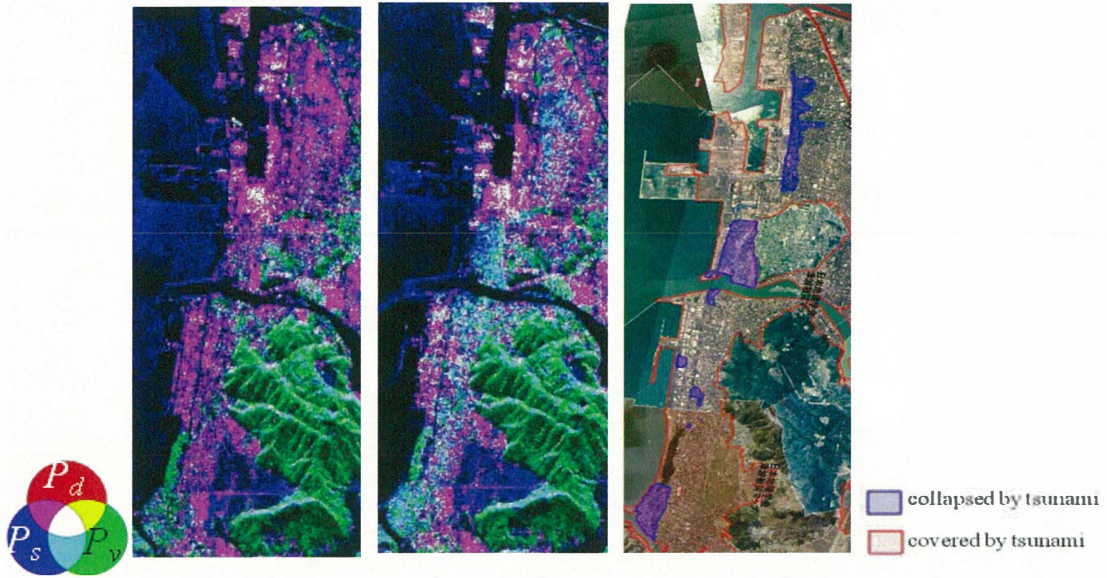
Off-Tohoku M9 Seaquake & Tsunami 110311



Off-Tohoku M9 Seaquake & Tsunami 110311



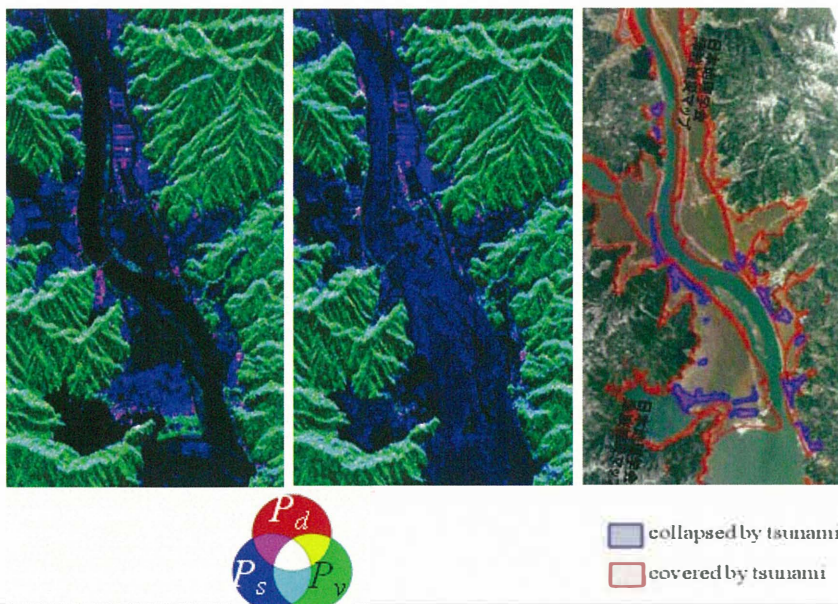
Off-Tohoku M9 Seaquake & Tsunami 110311



WIDEBAND INTERFEROMETRIC SENSING AND IMAGING POLARIMETRY

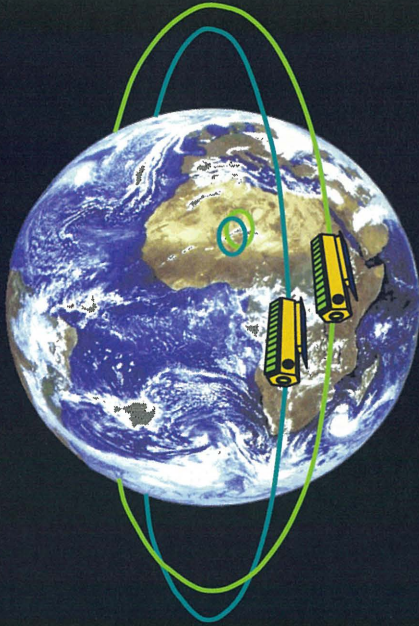
47

Off-Tohoku M9 Seaquake & Tsunami 110311



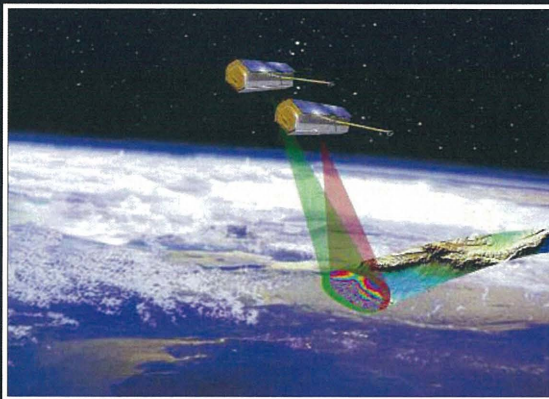
WIDEBAND INTERFEROMETRIC SENSING AND IMAGING POLARIMETRY

48



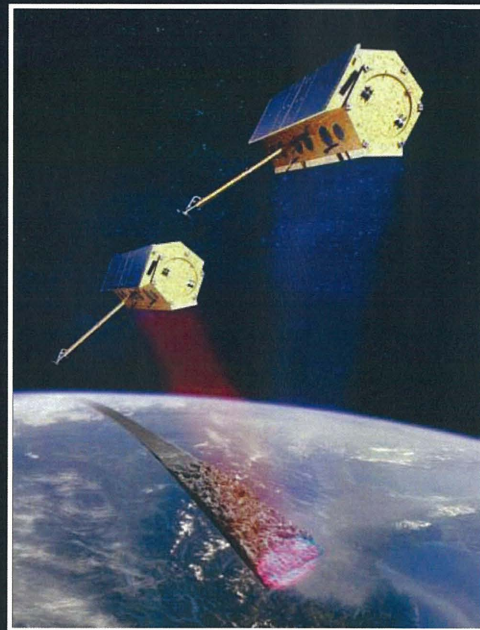
Global Monitoring of **Bio-**, **Geo-**, **Cryo-** and **Hydrosphere** processes with high temporal and spatial resolution.
(Prof. A. Moreira – POLINSAR09)

Radar Interferometry



TerraSAR – X (1 & 2)
(2010)

Pol – InSAR Sensors
TanDEM-X



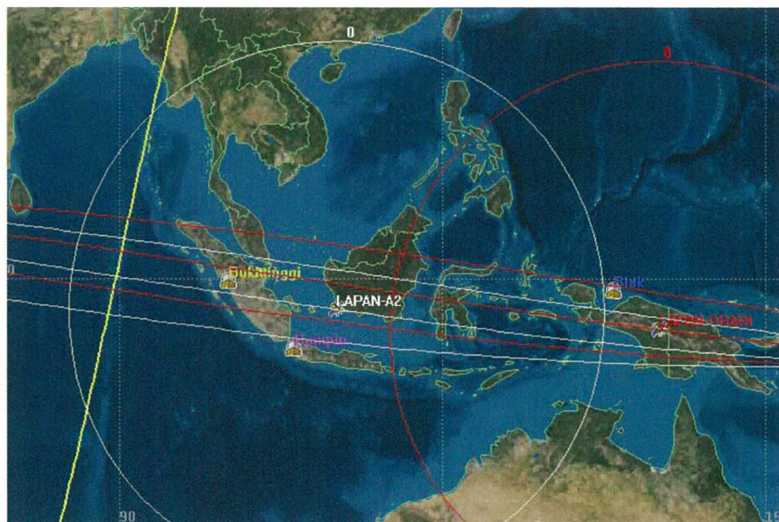
TandemSAR-L (Destiny): JPL & DLR



WIDEBAND INTERFEROMETRIC SENSING AND IMAGING POLARIMETRY

TUB-LAPAN-ORARI ORBIT PROFILE

(14 pass per 24 hr / orbit time 100 minutes and stay above horizon at about 10 minutes)



WIDEBAND INTERFEROMETRIC SENSING AND IMAGING POLARIMETRY

Major Paradigm for Remote Sensing from Air and Space of the Terrestrial Covers:

“Natural hazards are inevitable!
Natural disasters are not & how can we reduce aftereffects?”

Accomplished with the aid of fully Polarimetric POLinSAR Sensors at Very High Resolution and all pertinent bands:

ACQUISITION OF NEW BANDS FOR PASSIVE & ACTIVE SENSING

- | | |
|---|-----------------------|
| • Deep earth sounding | ULF - LF |
| • Ground penetrating radar | LF - VHF |
| • Mineral resource exploration | HF - UHF |
| • Biomass and vegetative cover estimation | HF – EHF (P/L/C-Band) |
| • Man made surface structure monitoring | HF – EHF (C/X/K-Band) |
| • Atmospheric passive remote sensing | cm – sub-mm |

- ◇ We need to put our act together as the global remote sensing community and request from ITU/WMO the protection of the “fundamental natural resource: the e-m spectrum”, and for providing the spectral bands for us to fulfill our professional duties as

“The Remote Sensing Pathologists and Radiologists of Earth and Planetary Covers”

Table - EESS (active) Frequency Bands between P-band and Ka-band (Huneycutt)

IEEE Band Designation	Frequency Band (MHz)	Bandwidth (MHz)	Allocation Status
P-band	432-438	6	Secondary (WRC'03)
L-band	1215-1300	85	Primary (WRC'97)
S-band	3100-3300	200	Secondary (WRC'97)
C-band	5250-5570	320	Primary (WRC'97)
X-band	8550-8650	100	Primary (WRC'97)
X-band	9300-9900	600	Primary (WRC'97, WRC'07)
Ku-band	13250-13750	500	Primary (WRC'97)
Ku-band	17200-17300	100	Primary (WRC'97)
K-band	24050-24250	200	Secondary (WRC'97)
Ka-band	35500-36000	500	Primary (WRC'97)

F-SAR technical characteristics (Reigber)

	X	C	S	L	P
RF [GHz]	9.6	5.3	3.25	1.325	0.35/0.45
Bw [MHz] PRF [kHz] PT [kW]	760	400	300	150	100/50
Rg res. [m] Az res. [m]	2.5	2.2	2.2	0.9	0.9
Rg cov. [km]	0.2	0.4	0.5	1.0	1.5
Sampling Channels Data rate	12.5 (at max. bandwidth)				
	8 bit real, 1000MHz				
	4	2	2	2	1
	247 MByte/s (per channel)				

FOUNDATIONS AND RELEVANCE OF MODERN EARTH REMOTE SENSING & ITS APPLICATIONS BY IMPLEMENTING SPACE-BORNE POL-IN-SAR

Conclusions:

The Electromagnetic **Vector (Polarization)**
Wave Spectrum:
A Natural Global Treasure

*Terrestrial Remote Sensing with POLinSAR for
The Diagnostics of the Health of the Earth*